Chapter 2

Experimental: Synthesis Procedure, Characterization and Measurements Details

2.1 Sample Synthesis

The **solid-state reaction route** is the most widely used method for the preparation of polycrystalline solids from a mixture of solid starting materials. Solids do not react together at room temperature over normal time scales and it is necessary to heat them to much higher temperatures, often to 1000 to 1500 °C in order for the reaction to occur at an appreciable rate. The factors on which the feasibility and rate of a solid state reaction include, reaction conditions, structural properties of the reactants, surface area of the solids, their reactivity and the thermodynamic free energy change associated with the reaction.

In solid state reaction technique, reactant chemicals were taken in required stoichiometric ratio and mixed thoroughly. After mixing, the solid mixture was heat treated at higher temperature for several hours with intermediate grindings. Prior to heat treatment, pelletization of samples are preferred since it increases the area of contact between the grains. Detailed process has been given in working chapters.

2.2 Experimental Tools & Their Working Principle

2.2.1 X- ray Diffraction

Diffraction can occur when any electromagnetic radiation interacts with a periodic structure. The repeat distance of the periodic structure must be about the same wavelength of the radiation. X-rays have wavelengths on the order of a few angstroms (1 Å = 0.1 nm). This is the typical inter-atomic distance in crystalline solids, making X-rays the correct order of magnitude for diffraction of atoms of crystalline materials. When X-rays are scattered from a crystalline solid they can constructively interfere, producing a diffracted beam.

Bragg's Law:

The relationship describing the angle at which a beam of X-rays of a particular wavelength diffracts from a crystalline surface was discovered by Sir William H. Bragg and Sir W. Lawrence Bragg and is known as Bragg's Law

$$2d\sin\theta = n\lambda \tag{2.1}$$

λ = wavelength of the x-ray

θ = scattering angle

n = integer representing the order of the diffraction peak

d = inter-plane distance of (i.e atoms, ions, molecules)

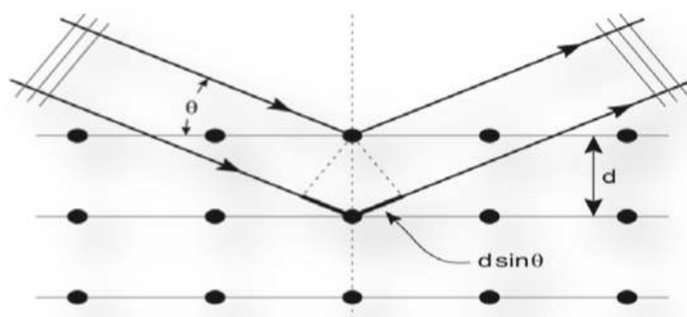

Fig. 2.1. *Schematic diagram of X-ray diffraction.*

X-ray pattern of a given powder sample is obtained by measuring the intensity with the variation of the angle (2θ). From the X-ray pattern following information can be obtained: Phase identification can be done by matching the XRD pattern with reference patterns (JCPDS–ICDD file) of pure substances. Quantitative information on single phase and multi-phase materials can be obtained using pattern calculation and pattern fitting methods (so-called Rietveld refinement). In combination with the use of standard materials, this approach can supply accurate values for sample composition, crystal symmetry, unit-cell dimensions, atom positions, site-occupancy factors and many more for pure as well as doped samples.

2.2.2 Neutron Diffraction

Neutron diffraction or **elastic neutron scattering** is the application of neutron scattering to the determination of the atomic and/or magnetic structure of a material: A

sample to be examined is placed in a beam of thermal or cold neutrons to obtain a diffraction pattern that provides information of the structure of the material. The technique is similar to X-ray diffraction but due to the different scattering properties of neutrons versus x-rays complementary information can be obtained.

2.2.3 Superconducting Quantum Interference Device

Superconducting quantum interference device is a mechanism used to measure extremely weak signals, such as changes in the human body's electromagnetic energy field. The superconducting quantum interference device (SQUID) consists of two superconductors separated by thin insulating layers to form two parallel Josephson junctions.

The device may be configured as a magnetometer to detect incredibly small magnetic fields -- small enough to measure the magnetic fields in living organisms. SQUIDs are sensitive enough to measure fields as low as 5×10^{-18} T. Their noise levels are as low as 3 f $T\cdot Hz^{-1/2}$.

Working principle

If a constant biasing current is maintained in the SQUID device, the measured voltage oscillates with the changes in phase at the two junctions, which depends upon the change in the magnetic flux. Counting the oscillations allows one to evaluate the flux change which has occurred.

A radio frequency (RF) SQUID is made up of one Josephson junction, which is mounted on a superconducting ring. An oscillating current is applied to an external circuit, whose voltage changes as an effect of the interaction between it and the ring. The magnetic flux is then measured.

A direct current (DC) SQUID, which is much more sensitive, consists of two Josephson junctions employed in parallel so that electrons tunneling through the junctions demonstrate quantum interference, dependent upon the strength of the magnetic field

within a loop. DC SQUID's demonstrate resistance in response to even tiny variations in a magnetic field, which is the capacity that enables detection of such minute changes.

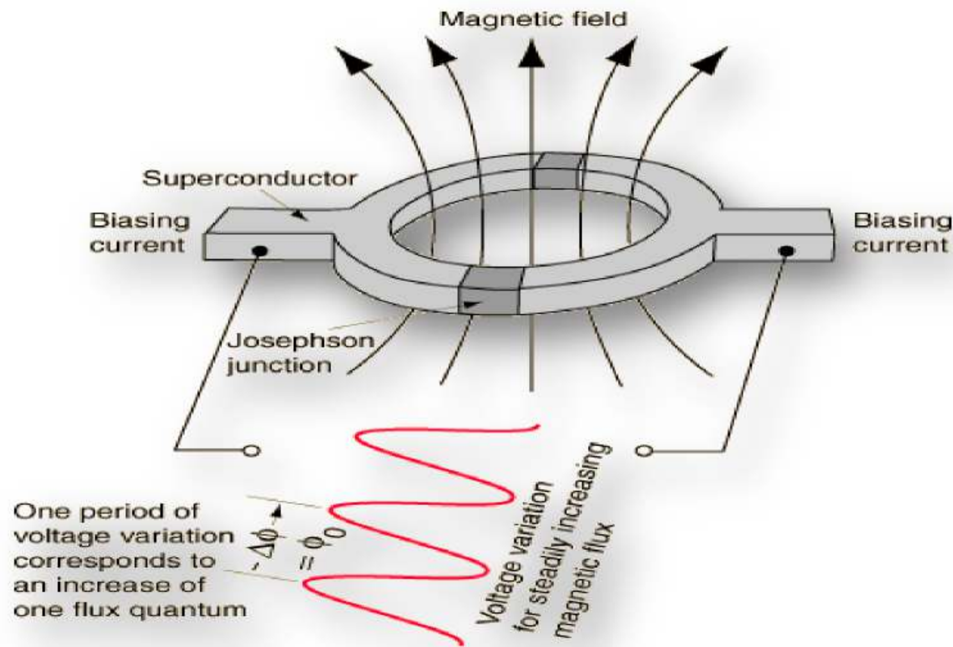

Fig. 2.2. *Josephson junction.*

The basic principle of operation is closely linked to flux quantization. This is the phenomenon that the favored states for a loop of superconductor are those where the flux inside is a multiple of the flux quantum.

$$\text{Flux quantum } (\Phi_0) = 2\pi\hbar/2e \cong 2.0678 \times 10^{-15} \text{ tesla} \times \text{m}^2 \quad (2.2)$$

where $\hbar = h/2\pi$ (h is planck constant) and e is electronic charge.

2.2.4 Transmission electron microscopy

The first electron microscope was built in 1932 by the German physicist Ernst Ruska, who was awarded the Nobel Prize in 1986 for its invention. Transmission electron microscopy (TEM) is a microscopy technique whereby a beam of electrons is transmitted

through an ultra thin specimen, interacting with the specimen as it passes through. An image is formed from the interaction of the electrons transmitted through the specimen; the image is magnified and focused onto an imaging device, such as a fluorescent screen, a sensor such as a CCD camera.

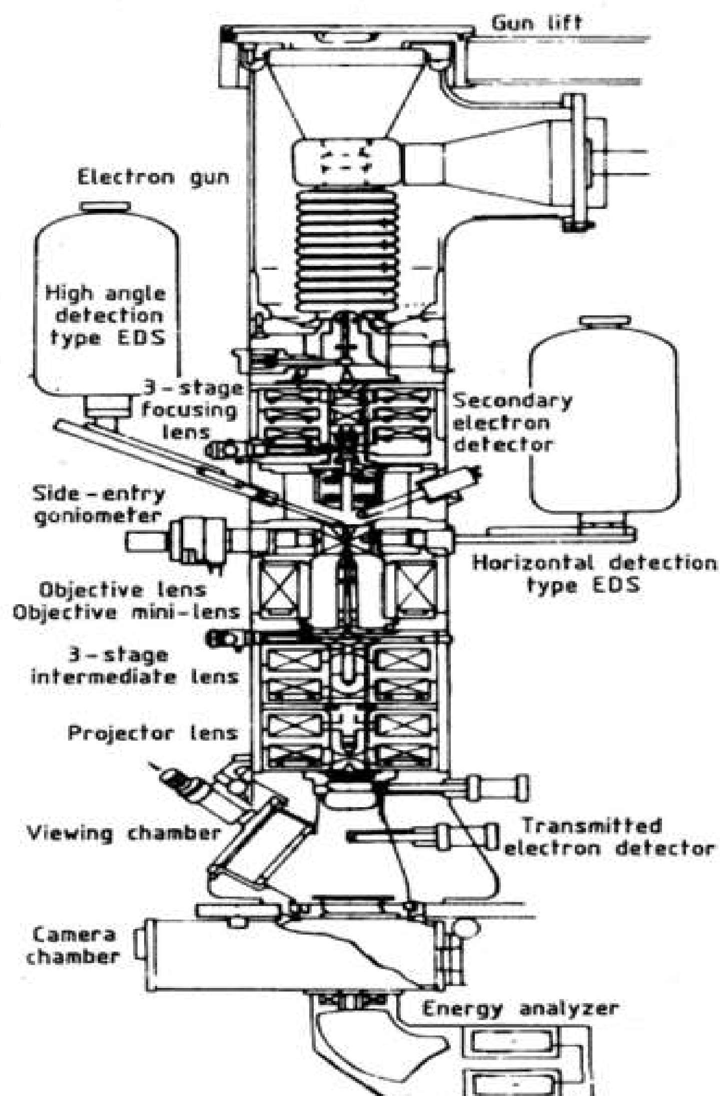

Fig. 2.3: *Layout of optical components in a basic TEM.*

TEM is composed of several components which include a vacuum system in which the electrons travel, an electron emission source for generation of the electron stream, a series of electromagnetic lenses, as well as electrostatic plates. TEM is capable of imaging at a significantly higher resolution than light. TEM forms a major analysis method in a range of scientific fields, in both physical and biological sciences. TEM find application in

cancer research, virology, materials science as well as pollution and semiconductor research. The specimen holders are adapted to hold a standard size of grid upon which the sample is placed or a standard size of self-supporting specimen. Standard size of TEM grid is a 3.05 mm diameter ring, with thickness and mesh size ranging from a few to 100 µm. The sample is placed onto the inner meshed area having diameter of approximately 2.5 mm. Generally, grid materials are copper, molybdenum, gold or platinum. This grid is placed into the sample holder which is paired with the specimen stage. A wide variety of designs of stages and holders exist, depending upon the type of experiment being performed.

Fig. 2.4. *Tecnai G^2 S-Twin (FEI, The Netherlands) Transmission Electron Microscope.*

Selected area electron diffraction (SAED) is an analytical technique that can be performed with TEM. In a TEM, a thin crystalline specimen is subjected to a parallel beam of high-energy electrons. As TEM specimens are typically ~100 nm thick, and the electrons typically have energy of 100-400 keV, the electrons pass through the sample easily. In this case, electrons are treated as wave-like, rather than particle-like because the wavelength of high-energy electrons

is a fraction of a nanometre, and the spacing between atoms in a solid is only slightly larger, the atoms act as a diffraction grating to the electrons, which are diffracted. That is, some fraction of them will be scattered to particular angles, determined by the crystal structure of the sample, while others continue to pass through the sample without deflection. As a result, the image on the screen of the TEM will be a series of spots (or ring like pattern). SAED patterns are a projection of the reciprocal lattice, with lattice reflections showing as sharp diffraction spots.

From the TEM micrograph following information can be obtained:

(i) The size and shape of the (nano)-particles can be estimated from low resolution TEM images.

(ii) SAED patterns can be used to identify crystal structures and to measure lattice parameters.

(iii) High-resolution TEM (HRTEM) gives the interplanar spacing (*d*-values).

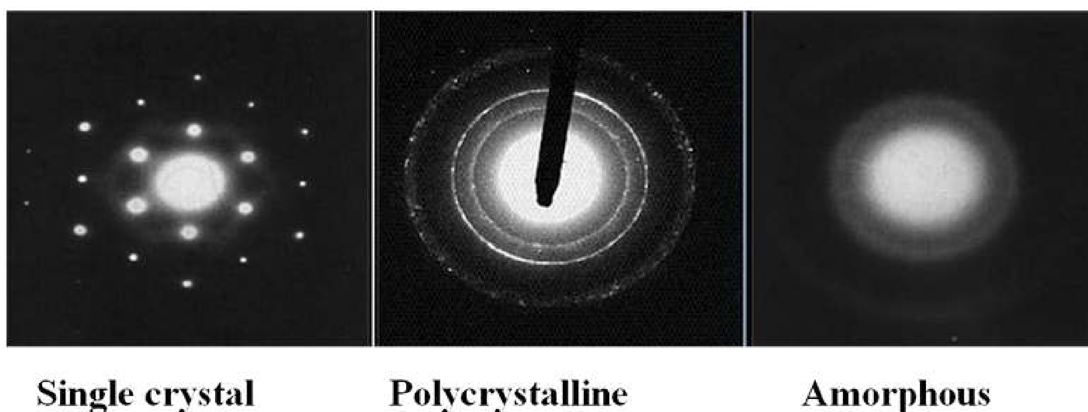

Fig. 2.5. *Selected area electron diffraction pattern of single crystal, polycrystalline and amorphous materials.*

2.2.5 X-ray Absorption Fine Structure (XAFS) Spectroscopy

X-ray absorption fine structure (XAFS) [1, 2] refers to the details of how X-rays are absorbed by an atom at energies near and above the core-level binding energies of that atom. Specifically, XAFS is the modulation of an atom's X-ray absorption probability due to the chemical and physical state of the atom. XAFS spectra are especially sensitive to the formal oxidation state, coordination chemistry, and the distances, coordination number and

species of the atoms immediately surrounding the selected element. Because of this dependence, XAFS provides a practical and relatively simple way to determine the chemical state and local atomic structure for a selected atomic species. XAFS can be used in a variety of systems and bulk physical environment. XAFS is being routinely used in a wide range of scientific fields, including biology, environmental science, catalysts research, and material science.

Since, XAFS is an atomic probe, it places few constraints on the sample that being studied. All atoms have core level electrons, and XAFS spectra can be measured for essentially every element on the periodic table. Importantly, crystallinity is not required for XAFS measurements, making it one of the few structural probes available for non-crystalline and highly disordered materials, including solutions. Because X-rays are fairly penetrating in matter, XAFS is not inherently surface-sensitive, though special measurement techniques can be applied to enhance its surface sensitivity. In many cases, XAFS measurements can be made on elements of minority and even trace abundance, giving a unique and direct measurement of chemical and physical state of dilute species in a variety of systems.

X-ray absorption measurements are relatively straightforward, provided one has an intense and energy-tunable source of X-rays. In practice, this usually means the use of synchrotrons, and the history and development of XAFS is closely parallel to that of synchrotron radiation. Many experimental techniques and sample conditions are available for XAFS, including such possibilities as very fast measurements of *in situ* chemical processes, high spatial resolution, and extreme conditions of temperature and pressure. Since, the characteristics of synchrotron sources and experimental station dictate what energy ranges, beam sizes, and intensities are available, this often puts practical experimental limits on the XAFS measurements that can be done even if there are few inherent limits on XAFS.

The X-ray absorption spectrum is typically divided into two regimes: X-ray absorption near-edge spectroscopy (XANES) [3] and extended X-ray absorption fine-structure spectroscopy (EXAFS). Though the two have the same physical origin, this distinction is convenient for the interpretation. XANES is strongly sensitive to formal oxidation state and coordination chemistry (e.g., octahedral, tetrahedral coordination) of the

absorbing atom, while the EXAFS is used to determine the distances, coordination number, and species of the neighbours of the absorbing atom.

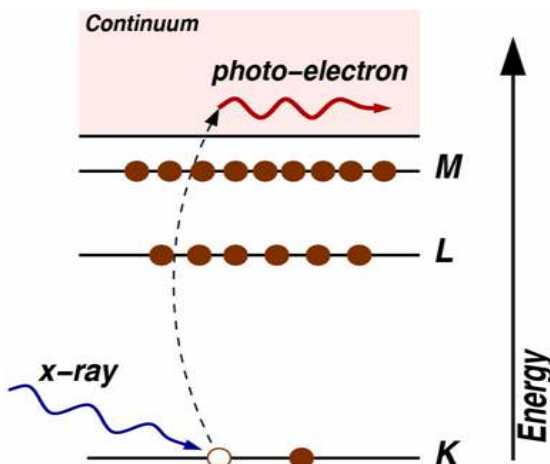

Fig. 2.6. *The photoelectric effect, in which an X-ray is absorbed and a core level electron is promoted out of the atom.*

X-rays are light with energies ranging from ~500 eV to 500 keV, or wavelengths from ~25 Å to ~0.25 Å. At this energy regime, light is absorbed by all matter through the photo-electric effect. In this process, an X-ray photon is absorbed by an electron in a tightly bound quantum core level (such as the 1s or 2p level) of an atom (Fig. 2.6).

In order for a particular electronic core level to participate in the absorption, the binding energy of this core level must be less than the energy of the incident X-ray. If the binding energy is greater than the energy of the X-ray, the bound electron will not be perturbed from the well-defined quantum state and will not absorb the X-ray. If the binding energy of the electron is less than that of the X-ray, the electron may be removed from its quantum level. In this case, the X-ray is destroyed (i.e., absorbed) and any energy in excess of the electronic binding energy is given to a photo-electron that is ejected from the atom. This process has been well understood for nearly a century (Einstein received the Nobel Prize for explaining this effect). The full implications of this process when applied to molecules, liquids, and solids will give rise to XAFS.

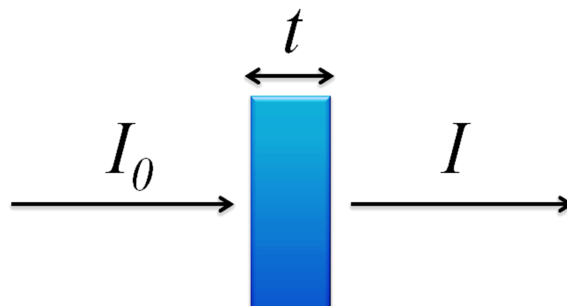

Fig. 2.7. *X-ray absorption measurements: An incident beam of monochromatic X-rays of intensity I_0 passes through a sample of thickness t, and the transmitted beam has intensity I.*

When discussing X-ray absorption, we are primarily concerned with the absorption coefficient 'μ' which gives the probability that X-rays will be absorbed according to Beer's Law:

$$I = I_0 e^{-\mu t} \tag{2.3}$$

where, I_0 is the X-ray intensity incident on a sample, 't' is the sample thickness, and I is the intensity transmitted through the sample, as shown in Fig. 2.7. For X-rays, as for all light, the X-ray intensity is proportional to the number of X-ray photons.

Following an absorption event, the atom is said to be in an excited state, with one of the core electron levels left empty (also called core hole), and a photo-electron. The excited state will eventually decay typically within a few femtosecond of the absorption event. Although this decay does not affect the X-ray absorption process, it is important for the discussion below.

There are two main mechanisms for the decay of the excited atomic state following an X-ray absorption event. The first of these is X-ray fluorescence (Fig. 2.8), in which a higher energy electron, i.e., core-level electron fills the deeper core hole, ejecting an X-ray of well-defined energy. The fluorescence energies emitted in this way are characteristic of the atom, and can be used to identify the atoms in a system, and to quantify their concentrations. For example, an L shell electron dropping into the K level gives the K_α fluorescence line.

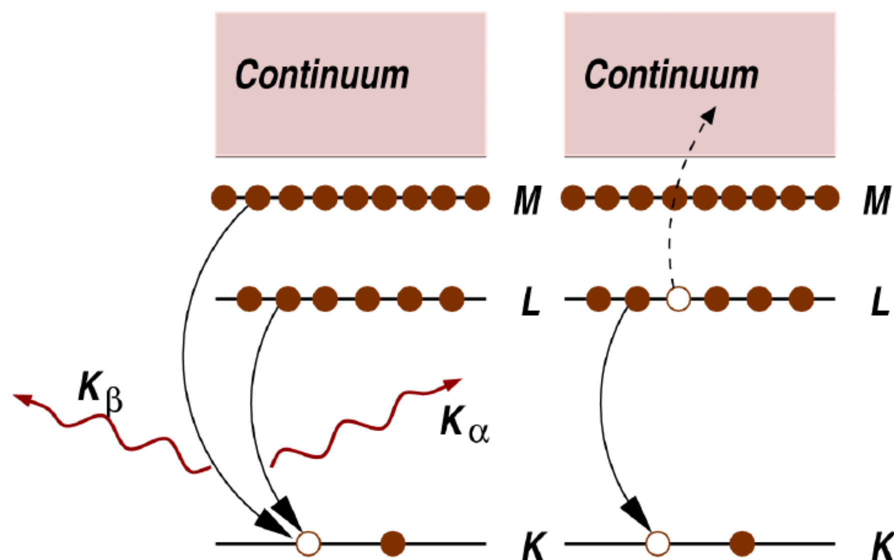

Fig. 2.8. *Decay of the excited state: X-ray fluorescence (left) and the Auger effect (right). In both cases, the probability of emission (X-ray or electron) is directly proportional to the absorption probability.*

The second process for de-excitation of the core hole is the Auger effect, in which an electron drops from a higher electron level and a second electron is emitted into the continuum (and possibly even out of the sample). In the hard X-ray regime (>2 keV), X-ray fluorescence is more likely to occur than Auger emission, but for lower energy X-ray absorption, Auger processes dominate. Either of these processes can be used to measure the absorption coefficient μ, though the use of fluorescence.

XAFS can be measured either in transmission or fluorescence geometries as shown in Fig. 2.7. (The geometry for Auger measurements is typically the same as for fluorescence). For now, it is enough to say that we can measure the energy dependence of the absorption coefficient $\mu(E)$ either in transmission as,

$$\mu(E) = \log \frac{I_0}{I} \tag{2.4}$$

or in X-ray fluorescence (or Auger emission) as,

$$\mu(E) \propto \frac{I_f}{I_0} \tag{2.5}$$

where, I_f is the monitored intensity of a fluorescence line (or, again, electron emission) associated with the absorption process.

A typical XAFS spectrum (measured in the transmission geometry for a powder of FeO) is shown in Fig. 2.9. The sharp rise in $\mu(E)$ due to the Fe 1s electron level (at 7112 eV) is clearly visible in the spectra, as are the oscillations in $\mu(E)$ that are the XAFS. As discussed earlier, the XAFS is generally thought of in two distinct portions: the near-edge spectra (XANES) - typically within 30 eV of the main absorption edge, and the extended fine-structure (EXAFS). The basic physical description of these two regimes is the same, but some important approximations and limits allow us to interpret the extended spectra in a more quantitative way than is currently possible for the near-edge spectra.

For the EXAFS, we are interested in the oscillations well above the absorption edge, and define the EXAFS fine-structure function $\chi(E)$, as

$$\chi(E) = \frac{\mu(E) - \mu_0(E)}{\Delta\mu_0(E_0)} \tag{2.6}$$

where, $\mu(E)$ is the measured absorption coefficient, $\mu_0(E)$ is a smooth background function representing the absorption of an isolated atom, and $\Delta\mu_0$ is the measured jump in the absorption $\mu(E)$ at the threshold energy E_0 (Fig. 2.9).

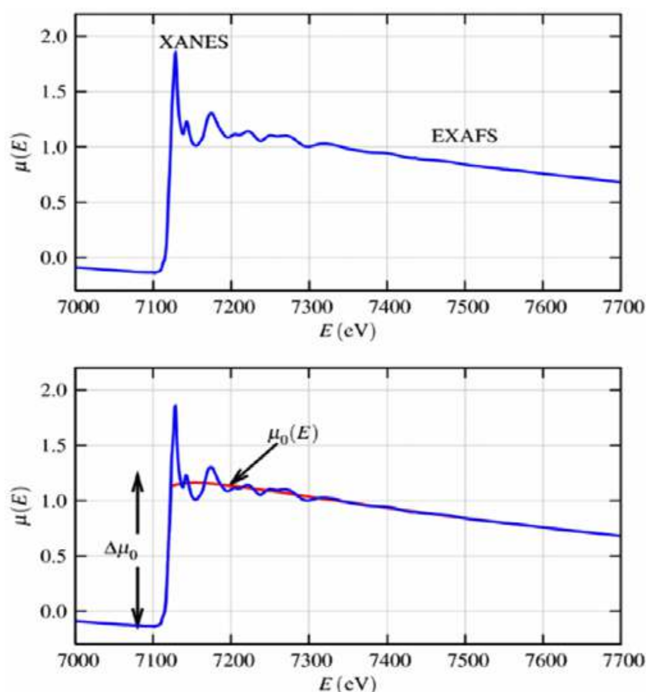

Fig. 2.9. *XAFS $\mu(E)$ for FeO. On top, the measured XAFS spectrum is shown with the XANES and EXAFS regions identified. On the bottom, $\mu(E)$ is shown with smooth background function $\mu_0(E)$ and the edge-step $\Delta\mu_0(E_0)$.*

2.2.6 Fourier Transform Infrared (FT-IR) Spectroscopy

Fourier transform infrared spectroscopy (FT-IR) is a technique which is used to obtain an infrared spectrum of absorption, emission, and Raman scattering, of a solid, liquid or gas. A typical FT-IR spectrometer simultaneously collects spectral data in a wide spectral range. This confers a significant advantage over another spectrometer which measures intensity over a narrow range of wavelengths at a time. FT-IR technique has made dispersive infrared spectrometers all and opened up new applications of infrared spectroscopy. The term Fourier transform infrared spectroscopy originates from the fact that a Fourier transform (a mathematical algorithm) is required to convert the raw data into the actual spectrum.

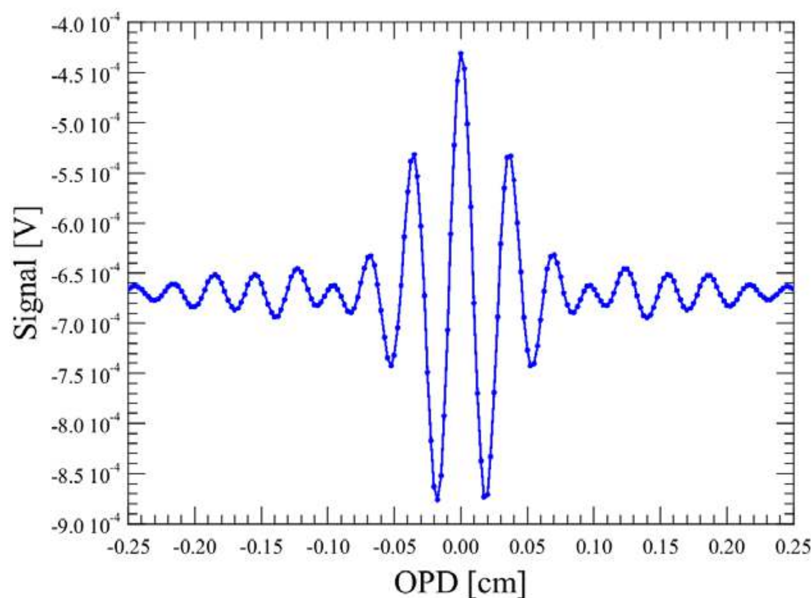

Fig. 2.10. *The centre burst of a sample interferogram from an FT-IR spectrometer.*

Fig. 2.11 shows an interferogram from an FT-IR spectrometer. The horizontal axis shows the position of the mirror, and the vertical axis shows the amount of light detected. This is the "raw data" which can be transformed into an actual spectrum.

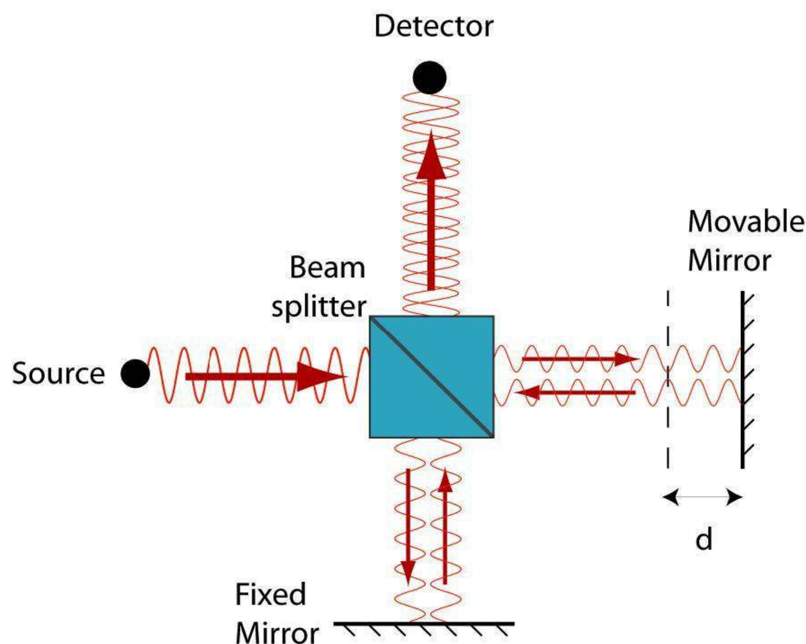

Fig. 2.11. *Schematic diagram of a Michelson interferometer, configured for FT-IR.*

The beam is generated by a light source-one containing the full spectrum of wavelengths to be measured. The light shines into a certain configuration of mirrors, called a Michelson interferometer that allows some wavelengths to pass through but block others. The beam is modified for each new data point by moving one of the mirrors; this changes the set of wavelengths that pass through.

In a Michelson interferometer adapted for FT-IR, light from the source, is collimated and directed to a beam splitter. Ideally, 50% of the light is reflected towards the fixed mirror and 50% is transmitted towards the moving mirror. Light is reflected from the two mirrors back to the beam splitter and (ideally) 50% of the original light passes into the sample compartment. There, the light is focused on the sample. On leaving the sample compartment, the light is refocused on to the detector. The difference in optical path length between the two arms to the interferometer is known as the retardation. An interferogram is obtained by varying the retardation and recording the signal from the detector for various values of the retardation. The form of the interferogram when no sample is present depends on factors such as the variation of source intensity and splitter efficiency with wavelength. This results in a maximum at zero retardation, when there are constructive interference at all wavelengths, followed by series of "wiggles". The position of zero retardation is determined accurately by finding the point of maximum intensity in the interferogram.

When a sample is present, the background interferogram is modulated by the presence of absorption bands in the sample.

There are two principal advantages for a FT-IR spectrometer compared to a scanning (dispersive) spectrometer.

1.The multiplex or Fellgett's advantage. This arises from the fact that information from all wavelengths is collected simultaneously. It results in a higher signal-to-noise ratio for a given scan-time or a shorter scan-time for a given resolution.

2.The throughput or Jacquinot's advantage. This results from the fact that, in a dispersive instrument, the monochromator has entrance and exit slits which restrict the amount of light that passes through it. The interferometer throughput is determined only by the diameter of the collimated beam coming from the source.

Other advantage includes less sensitivity to stray light, while a disadvantage is that FT-IR cannot use the advanced electronic filtering techniques that often makes its signal-to-noise ratio inferior to that of dispersive measurements.

Fig. 2.12. *Fourier transmission infrared spectrometer (Spectrum 65 FT-IR Spectrometer, Perkin Elmer Instrument, USA).*

2.2.7 Resistivity Measurement

Measuring the value of a resistor with an ohmmeter is pretty simple. You connect the meter to the resistor, and read off the measurement from the meter. But what if the

resistance you want to measure is very low (in the milli- or micro-ohm range)? In this case, the two-point method is not satisfactory because test contact resistance becomes a significant factor. A similar problem occurs, when making ground mat resistance tests, because long lead lengths (up to 1000 feet) are used. Here also, the lead resistance, due to long lead length, will affect the measurement results. The four-point resistance measurement method eliminates lead resistance or contact resistance.

An ohmmeter measures all resistance in the circuit loop, which includes the resistance of the wires connecting the ohmmeter to the component being measured. Such a scenario would be problematic if the connecting wires are very long, and/or the component to be measured has a very low resistance, and then the measurement error introduced by wire resistance will be substantial.

An ingenious method of measuring the subject resistance in a situation like this involves the use of both an ammeter and a voltmeter. We know from Ohm's Law that resistance is equal to voltage divided by current ($R = V/I$). Thus, we should be able to determine the resistance of the subject component if we measure the current going through it and the voltage dropped across it. Current is the same at all points in the circuit, because it is a series loop. Because we are only measuring voltage dropped across the subject resistance (and not the wire's resistances), though, the calculated resistance is indicative of the subject component's resistance alone.

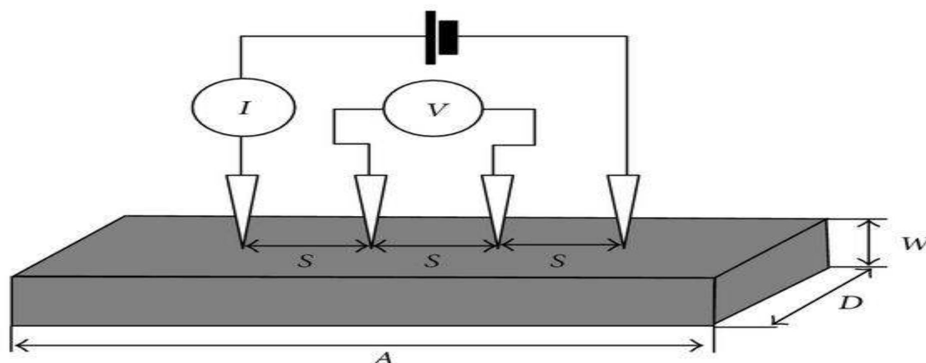

Fig.2.13. *Schematic diagram of test circuit for measuring resistivity with the four-point probe method.*

2.2.8 X-ray Photoemission Spectroscopy

X-ray photoelectron spectroscopy (XPS or ESCA) owes its quantification to Einstein's explanation of the photoelectric effect in 1905. X-ray photoelectron spectroscopy (XPS) is a quantitative spectroscopic technique that measures the elemental composition, empirical formula, chemical state and electronic state of the elements that exist within a material [4]. XPS spectra are obtained by irradiating a material with a beam of X-rays while simultaneously measuring the kinetic energy and number of electrons that escape from the top 1 to 10 nm of the material being analyzed. XPS requires ultra-high vacuum (UHV) conditions, typically ~10^{-10} torr. This facilitates the transmission of the photoelectrons to the analyzer but more importantly minimizes the re-contamination rate of a freshly cleaned sample.

In XPS, the sample is irradiated with low-energy (~1.5 keV) X-rays, in order to provoke the photoelectric effect. The energy spectrum of the emitted photoelectrons is determined by means of a high-resolution electron spectrometer.

A typical XPS spectrum is a plot of the number of electrons detected (sometimes per unit time) (Y-axis, ordinate) versus the binding energy of the electrons detected (X-axis, abscissa). Each element produces a characteristic set of XPS peaks at characteristic binding energy values that directly identify each element that exist in or on the surface of the material being analyzed. These characteristic peaks correspond to the electron configuration of the electrons within the atoms, e.g., 1s, 2s, 2p, 3s, etc. The number of detected electrons in each of the characteristic peaks is directly related to the amount of element within the area (volume) irradiated. To generate atomic percentage values, each raw XPS signal must be corrected by dividing its signal intensity (number of electrons detected) by a "relative sensitivity factor" (RSF) and normalized over all of the elements detected.

The electron binding energy of each of the emitted electrons can be determined by using an equation that is based on the work of Ernest Rutherford (1914):

$$E_{\mathrm{Binding}} = E_{\mathrm{Photon}} - (E_{\mathrm{Kinetic}} + \phi) \tag{2.7}$$

where $E_{Binding}$ is the binding energy (BE) of the electron, E_{Photon} is the energy of the X-ray photons being used, $E_{Kinetic}$ is the kinetic energy of the electron as measured by the instrument and ϕ is the work function of the spectrometer (not the material).

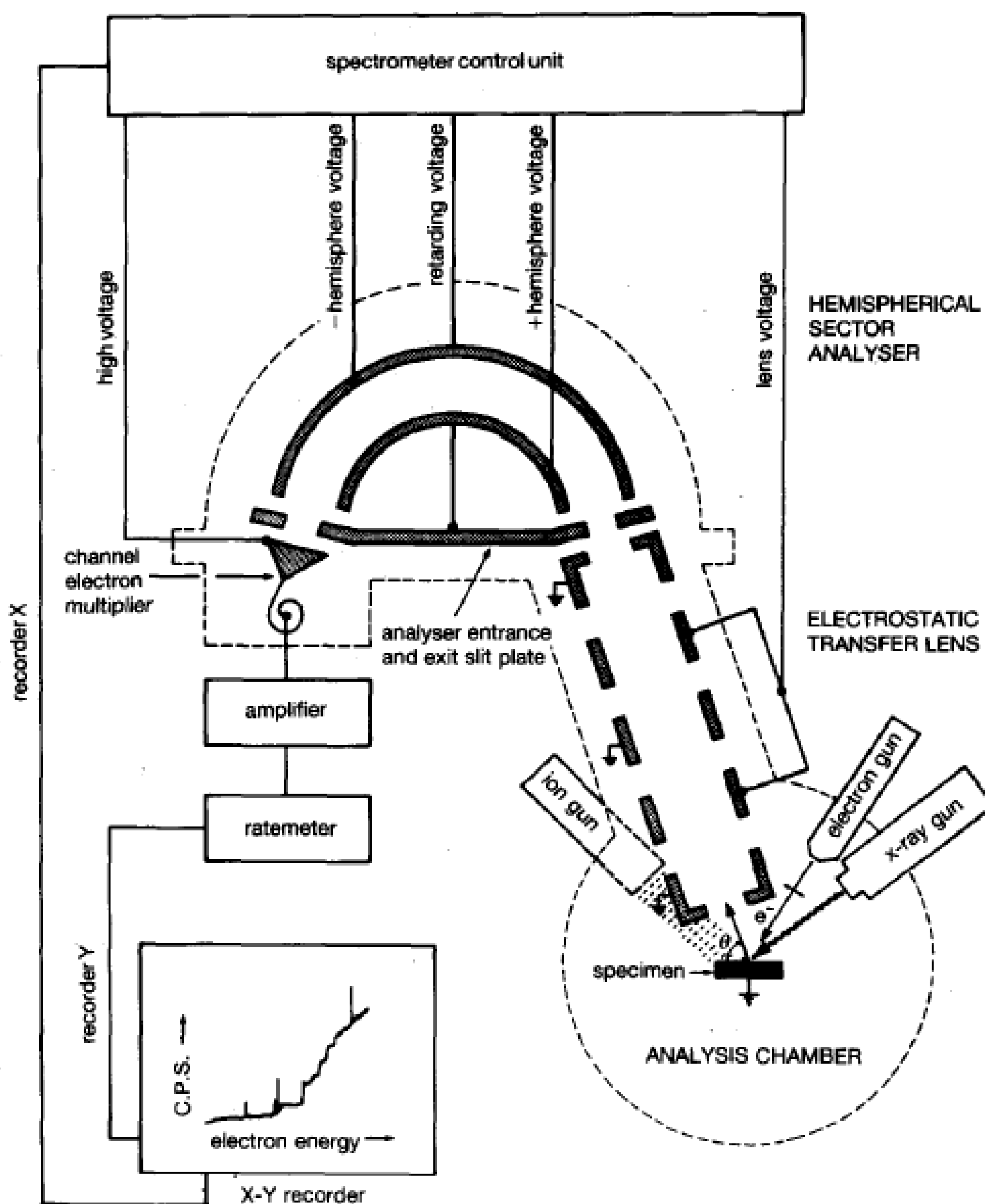

Fig.2.14. *Schematic diagram of X-ray photoemission spectroscopy.*

2.2.9 Thermoelectric Measurement

The **thermoelectric effect** is the direct conversion of temperature differences to electric voltage and vice-versa. A thermoelectric device creates a voltage when there is a different temperature on each side. Conversely, when a voltage is applied to it, it creates a temperature difference. At the atomic scale, an applied temperature gradient causes charge carriers in the material to diffuse from the hot side to the cold side; hence inducing a thermal current [5].

The **Seebeck effect** is the conversion of temperature differences directly into electricity. The thermopower or Seebeck coefficient, represented by S, of a material measures the magnitude of an induced thermoelectric voltage in response to a temperature difference across that material, and the entropy per charge carrier in the material. S has units of V/K, though μV/K is more common. If the temperature difference ΔT between the two ends of a material is small, then the thermopower of a material is defined approximately as:

$$S = -\frac{\Delta V}{\Delta T} \tag{2.8}$$

and a thermoelectric voltage of ΔV is seen at the terminals. Thermoelectric effect can be used as temperature sensing device and power generation device.

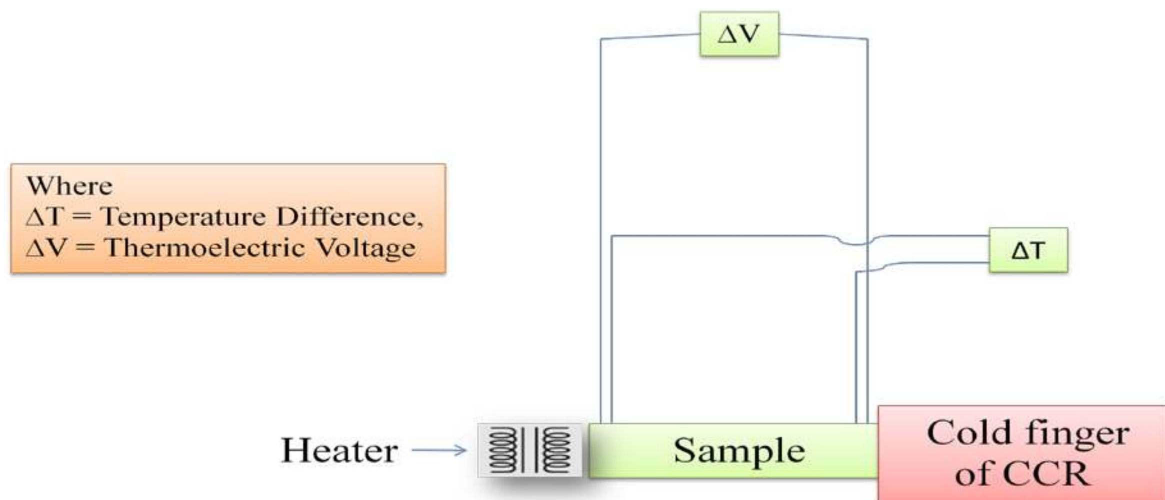

Fig. 2.15. *Block diagram of Thermoelectric measurement.*

2.2.10 AC Susceptibility

When we apply an AC magnetic field to the sample, it will cause a time dependent magnetization in the sample. In the limit of small AC field, we can express the induced AC moment as

$$M_{AC} = \left(\frac{dM}{dH}\right) H_{AC}(\omega t) \quad (2.9)$$

here, $H_{AC}(\omega t)$ is the oscillating magnetic field. and the susceptibility χ is given by

$$\chi = \frac{dM}{dH} \quad (2.10)$$

In the AC susceptibility measurement, the magnetic moment generates a dynamic response of the magnetic system of the sample. This can be studied by the complex response of the AC susceptibility

$$\chi = \chi' + i\chi'' \quad (2.11)$$

The real part describes the in-phase component with the field and the imaginary part is related with the out of phase component. Furthermore, the imaginary part is associated with the energy absorbed by the sample and it is given by

$$W = -2\pi\chi'' \frac{B^2}{2\mu_0} \quad (2.12)$$

The AC susceptibility measurement is a good tool to characterize the spin glass behavior, superparamagnetism and superconductivity.

References

[1]. Koningsberger, D. C. and Prins, R., X-ray absorption: Principles, applications, techniques of EXAFS, SEXAFS, and XANES, in Chemical Analysis 92, ed., John Wiley & Sons, 1988.

[2]. Newville, M., Fundamentals of XAFS, Consortium for Advanced Radiation Sources, University of Chicago, Chicago, IL, 2004.

[3]. Stern, E. A., Heald, S. M. and Koch, E. E., Principles and applications of EXAFS, Chapter 10 in Handbook of synchrotron radiation, ed., North-Holland, 1983.

[4]. Fadley, C. S., X-ray photoelectron spectroscopy: Progress and perspectives, Journal of Electron Spectroscopy and Related Phenomena 178-179, 2-32, 2010 and references therein.

[5]. Rowe, D. M., Thermoelectric waste heat recovery as a renewable energy source, Int. J. Inno. Energy Sys. Power 1, 12-23, 2006 and references therein.